e^+e^- Linear Colliders: Theoretical Basis and Perspectives

P.M. Zerwas

Deutsches Elektronen-Synchrotron DESY, D-22603 Hamburg / FRG

Abstract. The physics potential is summarized for e^+e^- linear colliders operating at center-of-mass energies up to $\sqrt{s} = 1\,\text{TeV}$ in the first phase, and at multi-TeV energies in the second phase. These machines will be ideal instruments to investigate the mechanisms for the breaking of the electroweak symmetries, the fundamental Higgs mechanism or dynamical alternatives. In supersymmetric theories, the spectrum of new particles and their interactions can be explored comprehensively and with high precision. The mechanism of supersymmetry breaking can be studied experimentally and the underlying fundamental theory can be reconstructed, eventually at scales near the Planck scale where particle physics and gravity are linked. The structure of space and time will be probed at distances down to $10^{-18}\,\text{cm}$ in scattering experiments. Precision studies of the electroweak gauge bosons, the top quark and QCD supplement the physics program of these machines.

I SYNOPSIS

Essential elements of the fundamental constituents of matter and their interactions have been discovered in the past three decades by operating electron-positron colliders. A coherent picture of matter has emerged that is adequately described by the Standard Model [1,2], in several of its sectors at a level of very high accuracy. However, the picture is still incomplete. The Higgs mechanism [3] which generates the masses of the fundamental particles in this model, has not been established yet experimentally though the indirect evidence is very strong and indications for a light Higgs boson have been observed recently.

Even if successfully completed, the Standard Model does not provide a comprehensive theory of matter. Neither the fundamental parameters, masses and couplings, nor the symmetry pattern can be explained, but these elements are merely built into the model. Moreover, gravity is not incorporated at the quantum level. First steps to solutions of these problems are associated with the unification of the electroweak and strong interactions [4], and with the supersymmetric extension of the Standard Model [5] which provides a stable bridge from the presently explored energy scales up to the grand-unification scale close to the Planck scale. This path to the linkage between particle physics and gravity is strongly supported by the successful prediction of the electroweak mixing angle.

An alternative path has recently received much attention. Extending space by extra dimensions which are compactified at distances of order 10^{-18} cm, the new space-time structure can be probed by scattering experiments at TeV energies.

Besides these novel phenomena, some facets of the Standard Model still await careful experimental analysis. This includes the top-quark properties and QCD, and the properties of the W electroweak bosons associated with the non-abelian symmetries of the gauge interactions. Moreover, remnants of extended grand-unified theories may generate new particles and forces in the lepton/quark and in the gauge-boson sector at the TeV scale.

While new high-mass vector bosons and particles carrying color quantum numbers can be searched for very efficiently at hadron colliders, lepton colliders provide in many ways unique opportunities to discover and explore non-colored particles. This is most obvious in the sector of electroweak symmetry breaking, described by the Higgs mechanism or dynamical symmetry breaking, as well as in supersymmetric theories. The Higgs boson of the Standard Model can be discovered at the hadron colliders Tevatron or LHC, yet the proper understanding of the mechanism for generating the masses of the fundamental particles can only be achieved at e^+e^- colliders. Moreover, the heavy Higgs bosons of supersymmetric theories can be found in only a small part of the parameter space at hadron colliders while the entire ensemble can be discovered at a multi-TeV e^+e^- collider. Squarks and gluinos can be searched for very efficiently at the Tevatron and LHC while the whole spectrum of colored and non-colored supersymmetric particles is accessible at e^+e^- colliders. Their properties can be analyzed very accurately in a model-independent way, just based on the well-defined kinematics of the subprocesses. The detailed knowledge of all the properties of the colored and non-colored supersymmetric states will experimentally reveal the mechanism of supersymmetry breaking and the structure of the fundamental supersymmetric theory near the Planck scale.

Thus, the physics program of e^+e^- linear colliders is in many aspects complementary to hadron machines. The high precision with which the properties of particles and their interactions can be explored, provides a solid platform from which extrapolations to new fundamental physics scales can be carried out, essential for reconstructing a comprehensive theory of matter and forces.

The LC program will likely be realized in two phases. In the first phase the c. m. energy range above LEP up to about 1 TeV will be covered in consecutive steps. High integrated luminosities of order 1 ab^{-1} and more provide the necessary base for the analyses described above. With typical cross sections of order 1 pb down to 1 fb, rates between 10^6 and 10^3 events can be generated within a year of operation. In the second phase of multi-TeV energies up to 5 TeV, the energy frontier can be explored in the après-LHC time. This physics program at high energies can be supplemented by the GigaZ mode, in which 10^9 Z bosons are generated in a year, and by operating the machine near the WW threshold. Electrons and positrons should be polarized at levels of 80 % and 60 % respectively, to allow for high-precision particle diagnostics.

Specific problems can be solved in the e^-e^-, $e\gamma$ and $\gamma\gamma$ modes of linear colliders. The same energies in e^-e^- or slightly reduced energies in $e\gamma/\gamma\gamma$ collisions can be reached, but luminosities are expected at the level of 20 % and 40 % of the corresponding e^+e^- luminosities. While standard (JLC/NLC) and superconducting (TESLA) technologies are presently studied for the first phase, multi-TeV energies require the development of a 2-beam accelerator (CLIC).

This report is built on the general reviews Refs. [6–8] and the material prepared for recent workshops [9–11] on the physics programs of e^+e^- linear colliders in the two consecutive phases. Many strategic and technical aspects not discussed in this report, are covered in the summary report of [12].

II THE HIGGS MECHANISM

The uncovering of the mechanism which breaks the electroweak symmetry $SU(2)_I \times U(1)_Y$ down to $U(1)_{EM}$ is one of the central problems to be solved by experiments at high energy accelerators [13,14]. Unitarity applied to quasi-elastic $WW \to WW$ scattering demands that either the electroweak bosons become strongly interacting particles at energies $\sqrt{s} > [4\pi\sqrt{G_F}]^{1/2} \approx 1.2\,\mathrm{TeV}$, or that a light, weakly interacting scalar Higgs boson should exist in Nature.

Within the standard approach, the Higgs mechanism is one of the building blocks of the electroweak interactions. The fundamental particles, leptons/quarks and electroweak gauge bosons, acquire masses by interacting with the scalar Higgs field in the ground state. To accommodate the well-established electromagnetic and weak phenomena, the Higgs mechanism requires at least one weak iso-doublet scalar field. After absorbing three Goldstone modes to build up the longitudinal polarization states of the $W^\pm$,Z bosons, one degree is left over which corresponds to a real scalar particle.

Three steps are necessary to establish the Higgs mechanism experimentally as the mechanism for generating the masses of the fundamental SM particles:

1. The Higgs boson must be discovered: the *experimentum crucis*;
2. The couplings of the Higgs particle with gauge bosons and fermions must be proven to increase with their masses;
3. The Higgs potential generating the non–zero Higgs field in the vacuum and breaking the electroweak symmetry in the scalar sector must be reconstructed by determining the Higgs self–couplings.

The only unknown parameter in the Higgs sector of the Standard Model is the the mass of the Higgs particle. Strong constraints on the mass can be derived, however, in two ways.

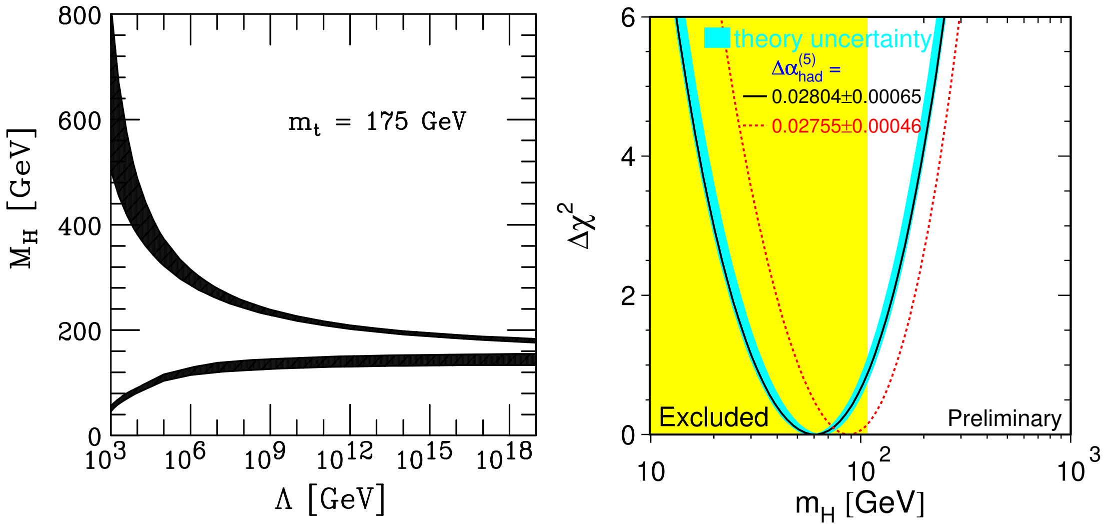

FIGURE 1. Left: Upper and lower bounds on the SM Higgs mass as a function of the scale parameter Λ for new strong interactions [15]. Right: Probability for the SM Higgs mass extracted from electroweak precision data [16].

A theoretical constraint can be derived from the upper scale Λ of the energy range in which the model is assumed to be valid before the particles become strongly interacting and new dynamical phenomena emerge [15]. Increasing the energy scale, the quartic self–coupling of the Higgs field grows for large values indefinitely. If the Higgs mass is small, the energy cut–off Λ is large at which the coupling grows beyond any bound. In particular, for a Higgs mass of less than 180 to 200 GeV, the Standard Model can be extended up to the scale of grand unification $\Lambda_{\rm GUT} \sim 10^{16}$ GeV, while all particles remain weakly interacting, cf. Fig. 1a. This hypothesis plays a key rôle in deriving the experimental value of the electroweak mixing parameter $\sin^2\theta_W \sim 0.2$ from grand unified theories. A light Higgs boson is therefore strongly preferred theoretically.

A second argument follows from the analysis of the electroweak precision data [16]. Radiative corrections to the W and Z propagators manifest themselves in the Fermi coupling and the electroweak mixing angle. While these corrections vary only logarithmically $\sim \alpha \log M_H^2/M_W^2$ [17], the accuracy of the electroweak data retains a crucial sensitivity on the Higgs mass. Including recent theoretical and experimental determinations of the electromagnetic coupling α, an upper limit of $M_H < 194$ GeV has been derived at the 95 % CL, see Fig. 1b.

It is quite important to notice that the constraint on the Higgs mass remains valid even if the Standard Model is modified by new strong physics scales Λ beyond 1 TeV [18]. In fact, if new strong interactions affect the SM particles in a plausibly large enough variety of modes, the compatibility with the electroweak precision data can be preserved only for a light Higgs boson mass $M_H \lesssim 400$ GeV.

By allowing for arbitrary values of the electroweak S, T, U parameters which describe deviations from the Standard Model in a purely phenomenological form, the electroweak data can be accounted for without introducing the Higgs boson [19]. However, no microscopic theory of dynamical symmetry breaking could be constructed so far, that would explain the small and negative S value in a natural way. Moreover, severe problems arise when fermion masses are introduced. The new interactions in extended schemes are characterized by scales of order $\sim 100\,\mathrm{TeV}$ and more to suppress flavor-changing neutral processes in the first two families, while scales must be restricted at the same time to the TeV range in order to generate the large masses of the t,b quarks in the third family.

A surplus of events has recently been observed at LEP experiments in the 4-jet channel and in the channel 2-jet + missing energy when the machine was operated at the highest possible energy above 206 GeV [20]. Since clearly identified b quarks have been isolated in the jets, these events are compatible with the expected Higgs signal for $M_H = 115.0^{+1.3}_{-0.9}\,\mathrm{GeV}$. However, with $2.9\,\sigma$, the rejection of the surplus as a possible statistical fluctuation or the increase of the significance to the $5\,\sigma$ level are reserved for future experiments. A general lower limit of $M_H \geq 113\,\mathrm{GeV}$ has been established by the LEP experiments.

In summary. Theoretical arguments and the analysis of the electroweak precision data favor a light Higgs boson, most likely in the intermediate mass range.

A The Higgs Boson of the Standard Model

The main production mechanisms for Higgs particles in e^+e^- collisions [21,22] are Higgs–strahlung off the Z boson line $e^+e^- \to ZH$ and the WW fusion process $e^+e^- \to \bar{\nu}\nu H$. With rising energy the Higgs–strahlung cross section scales $\sim \alpha_W^2/s$ while the fusion cross section increases logarithmically $\sim \alpha_W^3 M_W^{-2} \log s/M_H^2$, becoming dominant above 500 GeV:

$$\begin{aligned}
\sigma(e^+e^- \to ZH) &= \frac{G_F^2 M_Z^4}{96\pi s}\left[1+\left(1-4\sin^2\theta_W\right)^2\right]\beta\,\frac{\beta^2+12M_Z^2/s}{(1-M_Z^2/s)^2} \\
\sigma(e^+e^- \to \bar{\nu}\nu H) &\simeq \frac{G_F^3 M_W^4}{4\sqrt{2}\pi^3}\left[\left(1+\frac{M_H^2}{s}\right)\log\frac{s}{M_H^2}-2\left(1-\frac{M_H^2}{s}\right)\right]
\end{aligned}$$

with β denoting the 2-particle threshold function. The rates, about 10^5 events in one to two years of operation, are sufficiently large to detect Higgs particles with masses up to 70 % of the total e^+e^- c.m. energy. The recoiling Z boson in the two–body reaction $e^+e^- \to ZH$ is mono–energetic, $M_H^2 = s - 2\sqrt{s}E_Z + M_Z^2$, cf. Fig. 2, allowing high-precision measurements of the properties of the Higgs boson.

The mass of the Higgs boson can be measured very accurately by analyzing the recoil Z spectrum in Higgs–strahlung events. Experimental simulations have demonstrated that the error in the mass measurement can be reduced to $\delta M_H \lesssim$

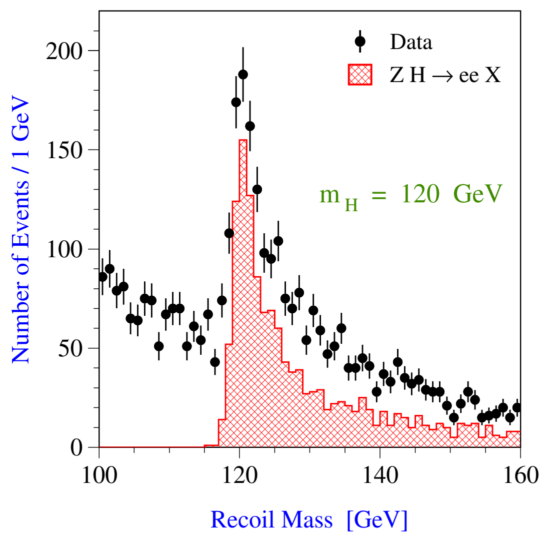

FIGURE 2. Production of the SM Higgs particle in the Higgs–strahlung channel $e^+e^- \to ZH \to e^+e^-X$; Ref. [9].

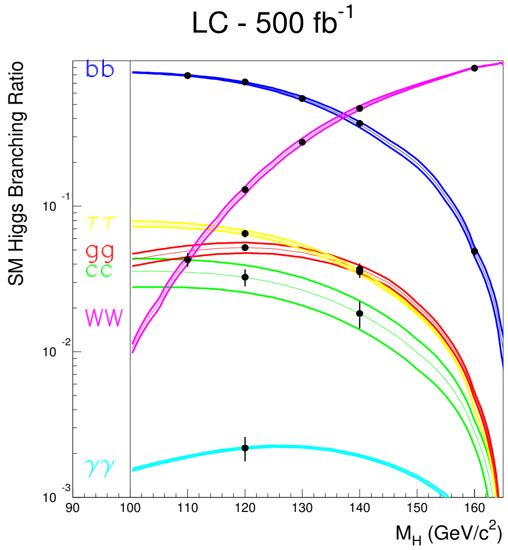

FIGURE 3. Branching ratios for decays of the SM Higgs boson; Ref. [14].

50 MeV in high–luminosity runs. The width of the SM Higgs boson can be determined in a nearly model–independent way in the difficult intermediate mass range in which the Breit–Wigner form cannot be reconstructed at an e^+e^- collider. Measuring the branching ratio BR_i in the decay and the partial width Γ_i in the production process, the total width Γ_H can be derived from $\Gamma_H = \Gamma_i/BR_i$. The channel $i = WW$ is very useful for this analysis [9], with the partial width Γ_{WW} extracted from the size of the WW fusion cross section.

The angular distribution of the Z/H bosons in the Higgs–strahlung process is sensitive to the external quantum numbers of the Higgs particle [23]. Since the amplitude is given by $\mathcal{A}(0^+) \sim \varepsilon_1 \cdot \varepsilon_2$, the Z boson is produced in a state of longitudinal polarization at high energies. As a result, the angular distribution $\mathrm{d}\sigma/\mathrm{d}\cos\theta \sim \beta \sin^2\theta + 8M_Z^2/s$ approaches the spin–zero law $\sin^2\theta$ asymptotically. This may be contrasted with the distribution $\sim 1 + \cos^2\theta$ for spinless negative-parity states. Higher spin assignments can be excluded by measuring the rise of the excitation curve $\sigma \sim \beta$ near the threshold and angular correlations involving the Z-decay fermions [24].

1 Higgs Couplings

Since the fundamental SM particles acquire masses through the interaction with the Higgs field, the scale of the Higgs couplings to fermions and gauge bosons is set by the masses of the particles:

$$g_{HVV} = 2M_V^2/v \qquad \text{and} \qquad g_{Hff} = M_f/v$$

It will be a very important task to measure the Higgs couplings to the fundamental particles since they are uniquely predicted by the very nature of the Higgs mechanism.

The Higgs couplings to massive gauge bosons can be determined from the measurement of the production cross sections, the HZZ coupling in the Higgs–strahlung and the HWW coupling in the fusion process. For Higgs couplings to fermions, the direct measurement of branching ratios $H \to b\bar{b}, c\bar{c}, \tau^+\tau^-$ can be exploited in the lower part of the intermediate mass range. This is exemplified in Fig. 3. By measuring the ratio of the $\tau\tau$ and cc to the bb branching ratios

$$\frac{BR(H \to \tau\tau)}{BR(H \to bb)} = \frac{m_\tau^2}{3m_b^2(M_H)} \qquad \text{and} \qquad \frac{BR(H \to cc)}{BR(H \to bb)} = \frac{m_c^2(M_H)}{m_b^2(M_H)}$$

the linear dependence of the Yukawa couplings on the masses of different fermion species can be tested very nicely. A direct way to determine the Yukawa coupling of the intermediate mass Higgs boson to the top quark in the range $m_H \leq 120$ GeV is provided by the bremsstrahlung process $e^+e^- \to t\bar{t}H$ in high energy e^+e^- colliders [25,9]. The absolute values of the Yukawa couplings can be reconstructed by combining decay branching ratios with the production cross sections.

2 *Higgs Potential*

To generate a non–zero value of the Higgs field in the vacuum, the minimum of the Higgs potential must be shifted away from the origin. Rewriting the potential

$$\begin{aligned} V &= \lambda\, [|\,\varphi\,|^2 - \tfrac{1}{2}\, v^2]^2 \\ &= \lambda v^2\, H^2 + \lambda v\, H^3 + \frac{\lambda}{4}\, H^4 \end{aligned}$$

in terms of the physical Higgs field H, the potential can be reconstructed by measuring the trilinear and quattrolinear couplings [26,27]. At a high–luminosity e^+e^- collider, the trilinear coupling can be tested in the double Higgs–strahlung process $e^+e^- \to Z + HH$. The splitting of a virtual Higgs boson into two real Higgs bosons is determined by the trilinear Higgs coupling: $e^+e^- \to Z + H^*\,[\to HH]$. Even though the cross section is less than 1 fb, the coupling can be measured nevertheless with an accuracy better than 20 % [28]. Thus an essential element of the mechanism responsible for the spontaneous symmetry breaking in the scalar sector can be established experimentally at a high–luminosity collider.

B SUSY Higgs Particles

The Higgs spectrum in the minimal supersymmetric extension of the Standard Model [29] consists of five states: h^0, H^0, A^0 and $H^{\pm}$. Besides the masses, two mixing angles define the properties of the scalar particles and their interactions with gauge bosons, fermions and the self–interactions: the ratio of the two vacuum expectation values $\mathrm{tg}\beta = v_2/v_1$ and a mixing angle α in the neutral CP–even sector. Supersymmetry leads to relations among the masses and mixing angles and, in fact, only two parameters are independent, which are generally chosen as the mass M_A and $\mathrm{tg}\beta$.

The search for the neutral SUSY Higgs bosons at e^+e^- colliders will be a straightforward extension of the search performed at LEP2. This collider has covered the mass range up to ~ 90 to 113 GeV for neutral Higgs bosons, depending on the value of $\mathrm{tg}\beta$. Higher energies, $\sqrt{s} \gtrsim 250$ GeV, are required to sweep the entire parameter space of the MSSM . The main production mechanisms of neutral Higgs bosons at e^+e^- colliders are the Higgs–strahlung process and associated pair production, as well as the related fusion processes. The cross sections for the four Higgs–strahlung and pair production processes can be expressed as

$$\begin{aligned} &(a)\ \textit{Higgs–strahlung}: && \sigma(e^+e^- \to Zh/ZH) = \sin^2(\beta-\alpha)/\cos^2(\beta-\alpha)\ \sigma_{SM} \\ &(b)\ \textit{Pair production}: && \sigma(e^+e^- \to Ah/AH) = \cos^2(\beta-\alpha)/\sin^2(\beta-\alpha)\ \bar{\lambda}\ \sigma_{SM} \end{aligned}$$

where σ_{SM} is the SM cross section for Higgs–strahlung and the factor $\bar{\lambda}$ accounts for the suppression of the P–wave cross sections near the threshold.

The cross sections for Higgs–strahlung and for pair production as well as the cross sections for the production of the light and the heavy neutral Higgs bosons h^0 and H^0 in association with either Z or A^0 are mutually complementary to each other, coming either with a coefficient $\sin^2(\beta-\alpha)$ or $\cos^2(\beta-\alpha)$. As a result, since σ_{SM} is large, at least the lightest CP–even Higgs boson will be accessible.

The cross section for hZ in the Higgs–strahlung process is large for values of M_h near the upper bound. The heavy CP–even and CP–odd Higgs bosons H and A, on the other hand, are produced pairwise [30] in this limit: $e^+e^- \to HA$. This decoupling limit corresponds to heavy Higgs masses above 250 to 300 GeV. The discovery limit for the heavy Higgs bosons is therefore set by the beam energy independently of the mixing parameter $\mathrm{tg}\beta$, in contrast to LHC where the heavy Higgs bosons cannot be detected individually in a large part of the parameter space.

The discovery range can be extended by searching for the resonance formation of Higgs bosons at a photon collider: $\gamma\gamma \to H$ and A. Higgs bosons with masses up to the maximum $\gamma\gamma$ invariant energy can be generated in this mode [31].

The charged Higgs bosons, if lighter than the top quark, can be produced in top decays, $t \to b + H^+$, with a branching ratio varying between 2 % and 20 % in the kinematically allowed region. Since for $\mathrm{tg}\beta$ larger than unity, the charged Higgs bosons will decay mainly into $\tau\nu_\tau$, this results in a surplus of τ final states over e, μ

final states in t decays, an apparent breaking of lepton universality. For large Higgs masses the dominant decay mode is the top decay $H^+ \to t\bar{b}$. In this case the charged Higgs particles must be pair produced [9] in e^+e^- colliders: $e^+e^- \to H^+H^-$. The cross section depends only on the Higgs mass. For small Higgs masses the cross section is of order 100 fb at $\sqrt{s} = 500\,\mathrm{GeV}$, but it drops very quickly due to the P–wave suppression $\sim \beta^3$ near the threshold.

The preceding discussion of the MSSM Higgs sector at e^+e^- linear colliders can be summarized in the following two points:
(i) The lightest CP–even Higgs particle h^0 can be detected in the entire range of the MSSM parameter space, either through the Higgs–strahlung process $e^+e^- \to Zh$ or through pair production $e^+e^- \to Ah$. In fact, this conclusion holds true even at a c.m. energy of 250 GeV, independently of the top and squark mass values, and also in scenarios in which invisible neutralino decays may occur.
(ii) The area in the parameter space where *all* SUSY Higgs bosons individually can be discovered at e^+e^- colliders is characterized by $M_A \lesssim \frac{1}{2}\sqrt{s}$, independently of tg$\beta$. Heavy H^0, A^0 Higgs bosons will be produced through Ah, AH associated production and charged Higgs bosons will be produced in H^+H^- pairs up to the kinematical limit. The entire Higgs spectrum can, therefore, be discovered at a multi-TeV e^+e^- collider.

A powerful no-lose theorem guarantees the discovery of the Higgs bosons also in extended supersymmetric models, including additional Higgs isosinglet or isodoublet fields. If the theory remains weakly interacting up to the GUT scale, the lightest Higgs mass will be below $\sim 200\,\mathrm{GeV}$. For sufficiently large mixing with the standard doublet, this Higgs boson will be generated by Higgs-strahlung. However, if this particle decouples, the second-lightest particle will effectively take over the rôle of the lightest Higgs boson, and the system will just be reduced by one degree of freedom. For the reduced system the same chain of arguments can be applied again, and repeatedly again until the MSSM level is reached for which the existence proof has been described above. Thus, at least one SUSY Higgs boson must be discovered even at a first-phase e^+e^- linear collider [32].

C Dynamical Electroweak-Symmetry Breaking

If the physical scenario in which W,Z,Higgs bosons are weakly interacting up to the GUT scale is not realized in Nature – despite of all the strong [but indirect] indications, the alternative scenario is a strongly interacting W sector [33]. Without a light Higgs boson with a mass less than about 1 TeV, the electroweak bosons must become strongly interacting particles at energies $\sim 1.2\,\mathrm{TeV}$ to comply with the requirements of unitarity for the W_LW_L scattering amplitudes. If the microscopic theory of the new strong interactions is endowed with a spontaneously broken chiral symmetry, the associated Goldstone bosons may be absorbed by the electroweak gauge fields to build up their longitudinal degrees of freedom. In fact, at high energies the longitudinally polarized electroweak bosons can be identified with the Goldstone bosons; in this way the strong interactions of the Goldstone bosons are transmitted to the electroweak boson sector.

This concept has exciting observable consequences at high-energy colliders. They can globally be characterized by the new strong interaction scale Λ_* which, as derived from loop expansions, must be of the order $\Lambda_* \simeq 4\pi v \lesssim 3\,\mathrm{TeV}$ or less.

(a) Anomalous contributions modify the non-abelian trilinear gauge-boson couplings which can be measured in W pair production at high energies: $e^+e^- \to \gamma, Z \to W^+W^-$. A high-luminosity e^+e^- collider at 500 GeV is sensitive [9] to any new strong-interaction scale Λ_* less than 3 TeV.

(b) Anomalous quattrolinear couplings can be measured in the same way through rescattering corrections in WW pair production. Sensitive to the (11) component of the (IJ) scattering phase shift, the Born production amplitude is supplemented by the Omnès rescattering amplitude

$$F = \exp \frac{s}{\pi} \int \frac{ds'}{s'} \frac{\delta_{11}(s')}{s' - s - i\varepsilon}$$

The other (IJ) components of the amplitudes α_{IJ} can be measured in WW scattering with the W bosons radiated off the initial electron and positron beams: $W^+W^- \to W^+W^-$ / ZZ in e^+e^- collisions, and $W^-W^- \to W^-W^-$ in e^-e^- collisions. In analogy to the $\pi\pi$ low-energy theorems, the first term in the energy expansion of the WW scattering amplitudes above the strong-interaction threshold is independent of dynamical details, just reflecting the spontaneous symmetry breaking, while the next term in the expansion [34] does depend on the structure of the new strong-interaction theory:

$$\mathcal{A}_{00} = +\frac{6s}{96\pi v^2}\left[1 + \alpha_{00}\frac{s}{\Lambda_*^2}\right] \qquad \mathcal{A}_{20} = -\frac{2s}{96\pi v^2}\left[1 + \alpha_{20}\frac{s}{\Lambda_*^2}\right]$$
$$\mathcal{A}_{11} = +\frac{s}{96\pi v^2}\left[1 + \alpha_{11}\frac{s}{\Lambda_*^2}\right]$$

The scattering amplitudes in the threshold region of the strong WW interactions can be tested to an accuracy of about 15 % at a high-luminosity collider of 1 TeV [35]. With $\alpha_{IJ} \sim 1$, the strong WW threshold region can be probed up to scales $\Lambda_* \lesssim 3\,\mathrm{TeV}$ [9].

The attractive $I = 0$ and $I = 1$ channels may form Higgs- and ρ-type resonances with masses $M \lesssim \Lambda_* \simeq 3\,\mathrm{TeV}$. The formation of these resonances [36] would lead to spectacular signals in WW collisions, cf. Fig. 4. In contrast to LHC with large jetty backgrounds, all these resonances can be fully reconstructed in the 4-jet final states [37] in a multi-TeV e^+e^- collider.

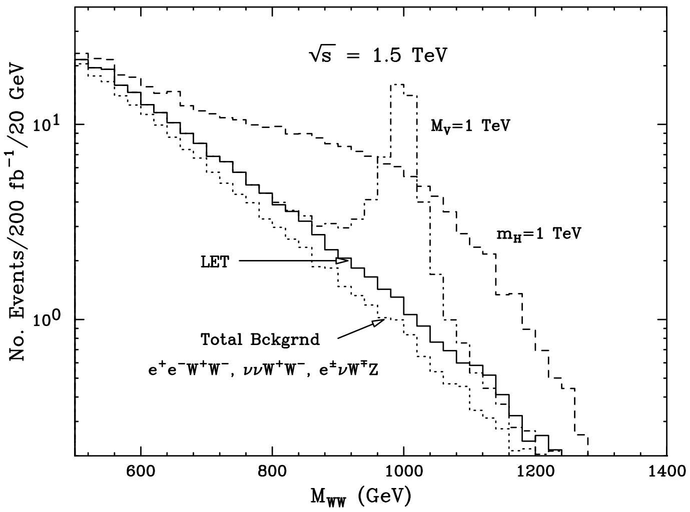

FIGURE 4. Signal of strongly interacting W^+W^- bosons in the TeV range for I =1 and 0 isospin channels; Ref. [36].

Strong enhancements would also be observed in $e^+e^- \to W^+W^-$ pair production through ρ-type resonances with mass $M_* \lesssim \sqrt{s}$, allowing for detailed measurements of the resonance parameters [9].

(c) Additional Goldstone bosons which are not absorbed by the electroweak gauge fields, may be observed as pseudo-Goldstone particles after acquiring masses of order 100 GeV. These particles can be searched for as resonance formation in $\gamma\gamma$ collisions, $\gamma\gamma \to P^0$, or in associate production with photons in e^+e^- collisions, $e^+e^- \to \gamma P^0$ [38].

Evidently, allowing the reconstruction of W bosons in jet final states as a result of the clean environment, e^+e^- linear colliders are unique machines for studying systems of strongly interacting electroweak W bosons. In the first phase, even at $\sqrt{s} = 500$ GeV, the entire WW threshold region is accessible for strong interaction scales up to the maximum scale $\Lambda_* \sim 3$ TeV. Parallel to the study of $\pi\pi$ scattering in ordinary QCD at low-energy colliders, the new strong interactions and the associated resonances can be studied in all details at a multi-TeV collider with energy in excess of 3 TeV.

III SUPERSYMMETRY

Even though there is no direct experimental evidence so far for the realization of supersymmetry in Nature, this concept has so many attractive features that it can be considered as a prime target of present and future experimental particle research. Arguments in favor of supersymmetry are deeply rooted in particle physics, and supersymmetry may play a key rôle in a quantum theory of gravity. In relating particles of different spins to each other, i.e. fermions to bosons, low–energy supersymmetry stabilizes the masses of fundamental Higgs scalars in the background of very high energy scales associated with grand unification. Besides solving this part of the hierarchy problem, supersymmetry may even be closely related to the physical origin of the Higgs phenomenon itself: In supergravity models, the evolution of one of the scalar masses squared from the GUT scale to the electroweak scale can become negative, giving rise to spontaneous symmetry breaking, if the top mass has a value between about 100 to 200 GeV while the electroweak sector $U(1)_{EM}$ and $SU(3)_C$ remains unbroken.

The minimal supersymmetric extension of the Standard Model is based on the SM group $SU(3) \times SU(2) \times U(1)$. The gauginos are the supersymmetric spin–$\frac{1}{2}$ partners of the gauge bosons. The quark and lepton matter particles are associated with scalar supersymmetric particles, squarks and sleptons. Two Higgs doublets are needed to endow down as well as up–type fermions with masses; the supersymmetric partners of the Higgs bosons are spin–$\frac{1}{2}$ higgsinos. [Charged/neutral higgsinos mix in general with the non–colored gauginos, forming charginos and neutralinos.] Supersymmetric partners carry a multiplicative quantum number $R = -1$ ($R = +1$ for ordinary particles) which is conserved in this model. Supersymmetric particles are therefore generated in pairs and the lightest supersymmetric particle LSP is stable.

Strong support for supersymmetry and the MSSM particle spectrum in the mass range of several hundred GeV follows from the high–precision measurement of the electroweak mixing angle $\sin^2\theta_W$. The value predicted by the MSSM and the value determined by the LEP and other experiments,

$$\begin{aligned} MSSM &: \quad \sin^2\theta_W = 0.2335 \pm 0.0017 \\ EXP &: \quad \sin^2\theta_W = 0.2310 \pm 0.0002 \end{aligned}$$

match surprisingly well, the difference being less than 2 per–mille.

The mass scale of supersymmetric particles is known only vaguely. As generic solution of the hierarchy problem, low-energy supersymmetry is characterized by a scale of order 1 TeV. Avoiding excessive fine tuning in the radiative corrections to the precision variables restricts the masses of the light charginos and neutralinos to typically less than 300 to 500 GeV [39]. The natural range for the LSP neutralino and right-chiral sleptons, derived from estimates of cold dark matter in the Universe, is 200 GeV and less [40]; however, it cannot be excluded that the LSP is much heavier in specific supersymmetric scenarios without overclosing the Universe. Attempts to explain the baryon asymmetry through CP violation in supersymmetric models [41], generally lead to light stop masses $\lesssim 150$ GeV, and low gaugino/higgsino parameters.

A central problem of supersymmetric theories is the breaking mechanism. Several scenarios have been proposed and experimental consequences have been elaborated in a few cases, in gravity mediated supersymmetry breaking mSUGRA and alternative scenarios [42]. Mass spectra of the supersymmetric particles are in general [43] quite different in different scenarios so that high–precision measurements of the particle properties will shed light experimentally on this theoretical problem. Moreover, extrapolations can be performed which will allow to reconstruct the basic supersymmetric theory eventually at a scale close to the Planck scale [44]. High–precision experiments at e^+e^- linear colliders [45] are expected to advance the understanding of supersymmetry in an essential way, and they may hold clues on the linkage between particle physics and gravity.

Supersymmetry will be explored in the two phases of e^+e^- colliders in three steps:

1. The comprehensive reconstruction of the entire spectrum of supersymmetric particles and the measurement of their properties, mass, spin, etc;
2. The extraction of the basic low-energy parameters: gaugino, higgsino and scalar mass parameters; mixings; gauge and Yukawa couplings;
3. The experimental analysis of supersymmetry breaking and the reconstruction of the fundamental supersymmetric theory.

A Supersymmetric Particles

Charginos and Neutralinos: The two charginos $\tilde{\chi}_i^+$ and the four neutralinos $\tilde{\chi}_i^0$, mixtures of the [non–colored] gauginos and higgsinos, are expected to be among the lightest supersymmetric particles. In the MSSM with conserved R–parity, the neutralino $\tilde{\chi}_1^0$ with the smallest mass, assumed to be the lightest supersymmetric particle altogether, is stable. The heavier neutralinos and the charginos decay into (possibly virtual) gauge and Higgs bosons plus the LSP, $\tilde{\chi}_i^0 \to \tilde{\chi}_1^0 + Z$ and $\tilde{\chi}_1^0 + W$, or if they are heavy enough, into neutralino/chargino cascades, and leptons plus sleptons.

Neutralinos and charginos are easy to detect at e^+e^- colliders. They are produced in pairs

$$
\begin{aligned}
e^+e^- &\to \tilde{\chi}_i^+\tilde{\chi}_j^- \qquad [i,j=1,2] \\
e^+e^- &\to \tilde{\chi}_i^0\tilde{\chi}_j^0 \qquad [i,j=1,..,4]
\end{aligned}
$$

through s–channel γ, Z exchange and t–channel selectron or sneutrino exchange. Since the cross sections are as large as $\mathcal{O}(100\text{ fb})$, enough events will be produced to discover these particles for masses nearly up to the kinematical limit.

The properties of the charginos and neutralinos can be studied in great detail at e^+e^- colliders [45]. From the fast onset $\sim \beta$ of the spin $-\frac{1}{2}$ excitation curve near the threshold, the masses can be measured very accurately within less than a hundred MeV. The decay spectra of heavier supersymmetric particles allow us to measure the mass of the LSP. Using polarized $e^{\pm}$ beams, the decomposition of the states into wino and higgsino components can be determined [46] since left–handed electrons couple to sneutrinos in the t–channel but right–handed electrons do not, so that the energy and angular dependence of the cross sections is different for the two polarization states. In a similar way the properties of neutralinos can be explored [47].

Sleptons and Squarks: The superpartners of the right–handed leptons decay into the associated SM partners and neutralinos/charginos. In major parts of the SUSY parameter space the dominant decay mode is $\tilde{\mu}_R \to \mu + \tilde{\chi}_1^0$. For the superpartners of the left–handed sleptons, the decay pattern is slightly more complicated since, besides the $\tilde{\chi}_1^0$ channels, decays into leptons and charginos are also possible. In e^+e^- [and e^-e^-] collisions, sleptons are produced in pairs:

$$e^+e^- \to \tilde{\mu}_L^+\tilde{\mu}_L^- \ , \ \tilde{\mu}_R^+\tilde{\mu}_R^- \ , \ \tilde{\nu}_L\bar{\tilde{\nu}}_L \ \ etc.$$

For charged sleptons, the production proceeds via γ, Z exchange in the s–channel, in the case of selectrons also by additional t–channel neutralino exchange. For sneutrinos, the process is mediated by s–channel Z exchange and, in the case of electron–sneutrinos, also by the t–channel exchange of charginos.

The cross sections for the pair production of sleptons are of the order of 10 to 100 fb so that their discovery is very easy up to the kinematical limit. From the P–wave onset $\sim \beta^3$ of the annihilation cross section the masses can in general be determined [45] at a level of 200 to 300 MeV; the sharper onset of selection production in e^-e^- scattering will reduce this number further. Enough events will be produced to study their detailed properties.

If one of the stop states is light enough due to the strong LR Yukawa mixing, these particles may be pair produced even at a 500 GeV collider:

$$e^+e^- \to \tilde{t}_i\overline{\tilde{t}_j} \qquad i,j = 1,2$$

By measuring the LR asymmetry of the production cross sections, the $\tilde{t}_L/\tilde{t}_R$ mixing angle can be determined to high accuracy $\delta \cos\theta_{\tilde{t}} \approx 0.01$ [48].

R-Parity: If the R-parity in supersymmetric theories is broken, three lepton-type particles may couple to each other. This could lead to spectacular resonance effects, e. g. in Bhabha scattering,

$$e^+e^- \to \tilde{\nu}_\tau \to e^+e^-$$

if the energy is sufficient to excite the scalar neutrino [9]. Equally polarized electrons and positrons disentangle the scalar resonance easily from a new heavy gauge boson.

Basic Parameters: From the precisely measured properties of the supersymmetric particles and their production and decay characteristics, the basic low-energy parameters can be extracted, typically with accuracies at the percent level [49]. Denoting the squared masses by the particle symbols, the parameters can easily be derived from the measured observables [50], for example

$$
\begin{aligned}
M_2/|\mu| &= \frac{1}{2}\left[2\left(\chi_2^c + \chi_1^c - 2W\right) \mp \left(\chi_2^c - \chi_1^c\right)\left(c_{2R} + c_{2L}\right)\right]^{1/2} \\
M_1^2 &= \sum \chi_i^0 - M_2^2 - \mu^2 - 2Z
\end{aligned}
$$

with $c_{2L} = \cos 2\phi_L$ etc for the mixing in the chargino (c) sector. The analysis can be extended to CP-violating supersymmetric theories in which μ and M_1 are complex mass parameters [46,49,51,52].

B Supersymmetry Breaking

The high precision with which masses, couplings and mixing parameters will be determined at e^+e^- colliders, can be exploited to test the mechanism for supersymmetry breaking and the structure of underlying theories. For several scenarios, experimental consequences have been derived in some detail: gravity mediated supersymmetry breaking mSUGRA [53]; gaugino mediated breaking $\tilde{g}$MSB [54]; gauge mediated breaking GMSB [55]; anomaly mediated breaking AMSB [56]; superstring driven breaking [57]; Scherk-Schwarz supersymmetry breaking SSSB [58].

The pattern of supersymmetric particle masses is generally quite characteristic for these models [43], yet ambiguities cannot be excluded *a priori*.

Additional characteristica are provided by decay patterns [9], following from the different hierarchies of masses and from the couplings. For instance, in GMSB the lightest neutralino or stau will decay into light gravitinos which will generate events with missing energy:

$$
\begin{aligned}
\tilde{\chi}_1^0 &\to \gamma + \tilde{G} = \gamma + \not{E} \\
\tilde{\tau}_1 &\to \tau + \tilde{G} = \tau + \not{E}
\end{aligned}
$$

In AMSB, on the other hand, the light chargino may be so close in mass to the light neutralino that the chargino decays are restricted to soft pions:

$$
\tilde{\chi}_1^\pm \to \tilde{\chi}_1^0 + \pi_{soft}^\pm
$$

These distinct decay patterns allow to single out specific SUSY breaking mechanisms quite efficiently.

C Reconstructing the Fundamental SUSY Theory

The reconstruction of the fundamental supersymmetric theory at high scales will be exemplified for minimal supergravity mSUGRA. If minimal supergravity with radiative electroweak symmetry breaking is the underlying theory, the observable properties of the superparticles can be expressed by a small set of parameters defined at the GUT scale. Basically four parameters specify the properties of the particles in the supersymmetric sector. The scalar mass parameter $\tilde{M}_0$, the $SU(2)$ gaugino mass $M_{1/2}$, the trilinear coupling A_0 and the sign of the coupling μ of the Higgs doublets in the superpotential, and $\tan\beta$, the ratio of the vacuum expectation values v_2/v_1.

Sum Rules: Since only a few parameters determine the low energy theory in the evolution from the GUT scale down to the electroweak scale, many relations can be found among the masses of the superparticles which can stringently be tested at e^+e^- colliders [59]. Two examples should illustrate the physics potential of the e^+e^- facilities in this context.

(i) The *gaugino masses* at the scale of $SU(2)\times U(1)$ symmetry breaking are related to the common $SU(2)$ gaugino mass $M_{1/2}$ at the GUT scale by the running gauge couplings:

$$M_i = \frac{\alpha_i}{\alpha_{GUT}} M_{1/2} \qquad i = SU(3), SU(2), U(1)$$

with α_{GUT} being the gauge coupling at the unification scale. The mass relation in the non–color sector $M_1/M_2 = 5/3\tan^2\theta_W \approx 1/2$ can be tested very well by measuring the masses and production cross sections of charginos and neutralinos.

(ii) In a similar way the *slepton masses* can be expressed in terms of a common scalar mass parameter $\tilde{M}_0$ at the GUT scale, contributions $\sim M_{1/2}$ due to the evolution from the GUT scale down to low energies, and the D terms related to the electroweak symmetry breaking. These expressions give rise to relations among the slepton masses:

$$\begin{aligned} m^2(\tilde{l}_L) - m^2(\tilde{\nu}) &= -(1-2\sin^2\theta_W)M_Z^2\cos 2\beta \\ m^2(\tilde{l}_L) - m^2(\tilde{l}_R) &= \kappa_L\, M_{1/2}^2 - \tfrac{1}{2}(1-4\sin^2\theta_W)M_Z^2\cos 2\beta \end{aligned}$$

with $\kappa_L = 0.37$. The second relation follows from the hypothesis that the scalar masses are universal at the GUT scale, in particular $\tilde{M}_0^2(\mathbf{5}^*) = \tilde{M}_0^2(\mathbf{10})$ within $SU(5)$. This assumption can be tested stringently by relating the mass difference between $\tilde{e}_L$ and $\tilde{e}_R$ to the $SU(2)$ gaugino mass.

Extrapolation to the High Scale: The most convincing algorithmic support for supersymmetry is presently given by the grand unification of the three gauge couplings at the GUT scale. Interpreted as the reconstruction of the grand-unified

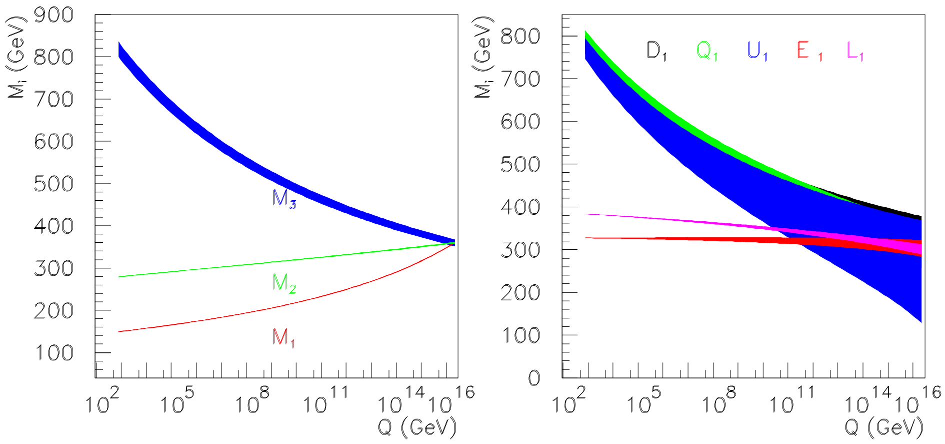

FIGURE 5. Example for the reconstruction of the fundamental supersymmetric mass parameters at the unification scale by evolution from the electroweak scale in the gaugino and scalar sectors; cf. Ref. [44].

gauge theory, a parallel evolution of the basic low-energy supersymmetric parameters should reveal the universality of these parameters at the high scale if mSUGRA is realized in Nature:

$$\begin{array}{llll} (a) & Gaugino\ masses : & M_1, M_2, M_3 & \rightarrow M_{1/2} \\ (b) & Scalar\ masses : & \tilde{M}_L^2, \tilde{M}_Q^2\ etc & \rightarrow \tilde{M}_0^2 \end{array}$$

Since the evolution is based solely on low-energy parameters, the reconstruction [44] of the universal gaugino and scalar masses is bias-free. In particular, pseudo-fixed point structures become visible operationally so that the confidence level with which the fundamental supersymmetric theory at the high scale can be reconstructed, cf. Fig. 5, is apparent.

Other scenarios can be discriminated from mSUGRA by studying the extrapolation to the high scale. For example, in GMSB the scalar mass parameters do not unify, but instead masses associated with particles carrying the same quantum numbers, are proven to be equal at the intermediate GMSB scale [44].

An *a postiori* fit, cf. Table 1, based on LC data, improves the knowledge of the mSUGRA parameters by an order of magnitude compared to a corresponding LHC analysis [50].

In summary. Precision tests of supersymmetric particles in e^+e^- collider experiments can open a window to energy scales close to the Planck scale. Supplemented by cosmological observations, these analyses give access to the area where gravity, the fourth of the fundamental forces, becomes an integral part of physics.

TABLE 1. *Measurement of universal mSUGRA parameters [50].*

Parameter	Theor. Value	Meas. Error
m_0	100 GeV	0.09 GeV
$M_{1/2}$	200 GeV	0.10 GeV
A_0	0 GeV	6.30 GeV
$\tan\beta$	3	0.02

IV SPACE-TIME STRUCTURE

Novel approaches have recently been proposed [60] to solve the hierarchy problem of the standard scenario between the Planck scale, the apparent scale where gravity becomes strong, and the electroweak scale of particle physics. Several avenues have been followed in this context, with the common feature that space is extended by extra dimensions which are compactified at a scale R. The fundamental scale M_G of quantum gravity, the standard Planck scale M_{PL}, and the scale R are related by

$$M_{PL}^2 = M_G^{2+N} R^N$$

for N extra space dimensions.

A The maxi/midi/mini Parade

Depending on the size of M_G and R, different scenarios have been proposed which can be investigated in high-energy experiments [43]. The scenarios sketched below are a few representative examples for much wider classes of potential structures beyond Minkowski space.

maxi: In this scenario, the energy scale M_G is close to the electroweak scale in the (multi-) TeV range [61]. While gravity extends over 4+N dimensions, the SM fields are restricted to a 3+1 dimensional brane or wall. Gravity appears weak as only the 4-dimensional projection is operative on the SM wall. Since M_G is small, the scale R can be large, i. e. even of semi-macroscopic size.

On the compactified space, the gravitational field generates a tower of equally and densely spaced Kaluza-Klein states with masses $M_n = n/R$. Two types of experiments can probe such a scenario [62,63]:
(i) Graviton emission: $e^+e^- \to \gamma + G_{KK} = \gamma + \not{E}$
For four extra dimensions scales M_G up to ~ 4 TeV can be probed in the first phase and up to 20 TeV in the second phase of linear colliders.

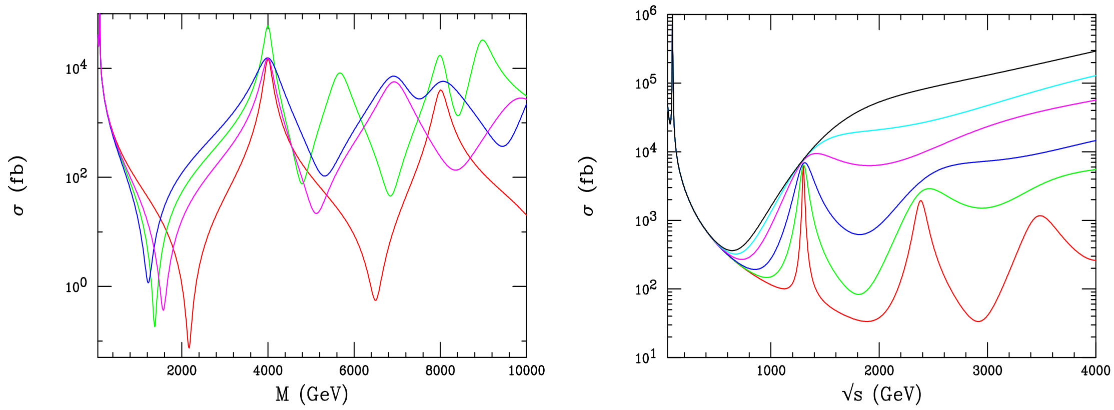

FIGURE 6. Left: Cross section for the effect of KK gauge-boson towers on the process $e^+e^- \to \mu^+\mu^-$ with $d = 2$ assuming $M_1 = 4\,\text{TeV}$; the red (green, blue, purple) curve corresponds to the S^1/Z_2 ($Z_2 \times Z_2$, $Z_{3,6}$, S^2) compactifications. Right: Cross section for $e^+e^- \to \mu^+\mu^-$ including the exchange of KK gravitons, taking the mass of the first mode to be 1.3 TeV, as a function of energy. From top to bottom the curves correspond to c =1.0, 0.7, 0.5, 0.3, 0.2 and 0.1. Ref. [65].

(ii) Graviton exchange: $e^+e^- \to f\bar{f}$
The exchange of a graviton KK tower [62–64] between the initial e^+e^- and the final $f\bar{f}$ state can effectively be described as a spin-2 contact interaction. Sensitivities to scales of order 8 TeV and 40 TeV in the first/second collider phase are expected. Moreover, the spin-2 character of gravity effects manifests itself in the angular distributions.

midi: In scenarios in which R is order TeV^{-1}, KK towers of gauge fields may be observed in high-energy experiments, characterized by masses of order TeV and beyond. They manifest themselves as a spectacular sequence of TeV resonances in reactions like $e^+e^- \to \mu^+\mu^-$, cf. Fig. 6/left.

mini: If the hierarchy is generated by an exponential warp factor arising from a 5-dimensional non-factorizable geometry, the gravity scales, i. e. Planck scale M_{PL}, 5-dimensional Planck scale M_G, curvature parameter k and r_c, are all qualitatively of similar magnitude [66]. If gravity is localized on one brane, the TeV scale can be generated on the second, SM brane at the distance r_c by $\Lambda = M_{PL} e^{-k r_c \pi}$, which is of order TeV for $k\,r_c \sim 11$ to 12. Since gravity is defined on a compactified space, KK towers of graviton states with masses of order TeV will be found, giving rise to resonant scattering at high energies, cf. Fig. 6/right, characteristic for a given ratio $c = k/M_{PL}$ between 1 and ~ 0.1.

Thus, TeV lepton colliders can provide previously unexpected information on the structure of space and time. Colliders at the multi-TeV energy frontier are unique in sensitivity, the precision reached in angular distributions at all phases of these machines is highly important for analyzing the dynamics realized on the extra space dimensions.

V ELECTROWEAK GAUGE BOSONS

A Standard W, Z Bosons

The fundamental electroweak and strong forces appear to be of gauge theoretical origin. This is one of the outstanding results of theoretical and experimental analyses in the past three decades. However, little direct evidence has been accumulated so far for the non–abelian nature of the forces in the electroweak $W^{\pm}, Z, \gamma$ sector. Since deviations from the gauge symmetries manifest themselves in experimental observables at least with coefficients $(\beta\gamma)^2$, high energies will allow stringent direct tests of the self–couplings of the electroweak gauge bosons.

The gauge symmetries of the Standard Model determine the form and the strength of the self–interactions of the electroweak bosons, triple couplings $WW\gamma, WWZ$ and quartic couplings. Deviations from the gauge-symmetric form of these vertices could be expected in more general scenarios. In models in which W, Z bosons are generated dynamically and interact strongly with each other at high scales Λ, corrections could alter the vertices to order $(v/\Lambda)^2$ and induce new types of couplings.

The properties of the Z boson have been studied at LEP and SLC with very high accuracy. By operating a linear collider at low energies on the Z resonance in the GigaZ mode, and near the WW threshold, the measurement of the fundamental electroweak parameters, mixing angle and W mass, can be improved by yet an order of magnitude, allowing to test electroweak symmetry breaking stringently at the quantum level.

The GigaZ Mode: By building a bypass for the transport of electron and positron bunches at TESLA, for instance, high luminosity can also be reached at low energies. On the Z resonance, an ensemble of 10^9 events, 1 GigaZ, can be generated in a year, expanding the LEP sample by two orders of magnitude. With both electron and positron beams longitudinally polarized, the electroweak mixing angle can be determined very accurately by measuring the left–right asymmetry [67]: $A_{LR} = 2\,(1 - 4\sin^2\theta_W)\;/\;[1 + (1 - 4\sin^2\theta_W)^2]\,:\,\delta\sin^2\theta_W \approx 10^{-5}$.

Similarly the measurement of the W mass can be improved to $\delta M_W \approx 6\,\mathrm{MeV}$ by scanning the threshold region [68].

Based on these two measurements, many high–precision tests can be performed in the electroweak sector. Extracting the Higgs mass from the electroweak observables is particularly interesting. From the ρ–parameter [69] this mass can be predicted to an accuracy of about 6%, improving LHC based predictions by almost an order of magnitude. Comparing this prediction with the direct measurement of the Higgs mass, quantum fluctuations can be tested stringently in a spontaneously

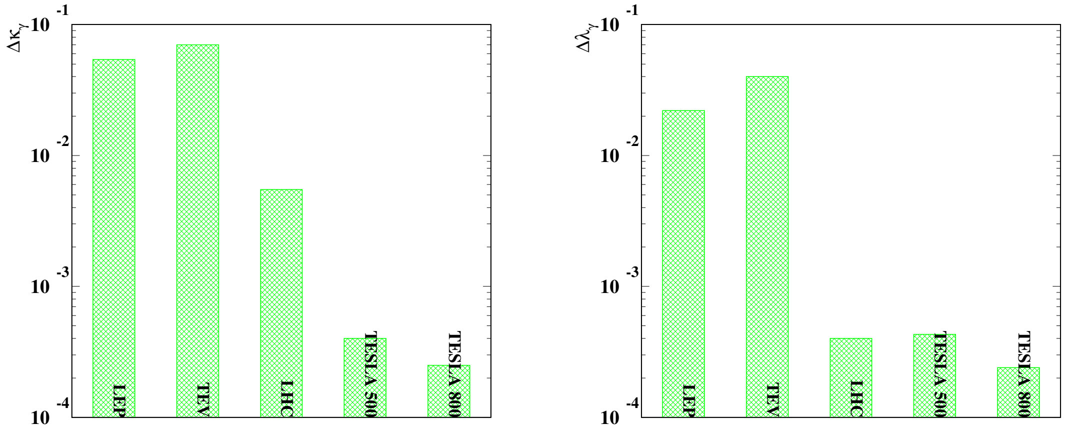

FIGURE 7. Constraints on anomalous trilinear couplings of electroweak bosons measured or expected at hadron colliders, LEP and TESLA [9].

broken gauge theory.

The Triple Gauge Boson Couplings: The couplings $W^+W^-\gamma$ and W^+W^-Z are in general described each by seven parameters. Assuming $\mathcal{C}, \mathcal{P}$ and $\mathcal{T}$ invariance in the pure electroweak boson sector, the number of parameters can be reduced to three, which can be identified with the γ, Z charges of the W bosons and the related magnetic dipole moments and electric quadrupole moments. They can be measured through the production of WW pairs at e^+e^- and $\gamma\gamma$ colliders. Detailed experimental analyses have been carried out for the reaction $e^+e^- \to W^+W^- \to (l\nu_e)(q\bar{q}')$. The bounds on $\Delta\kappa, \lambda$ which can be obtained at e^+e^- colliders of 500 GeV [9] are significantly better than the bounds expected from the LHC, reaching levels of less than 10^{-3}. Moreover, they improve at 1 TeV by nearly an order of magnitude, cf. Fig. 7. The analysis can be extended to quartic couplings [70]; anomalies would become visible for new strong interaction scales close to 1 TeV.

B Extended Gauge Theories

The gauge symmetry of the Standard Model, $SU(3) \times SU(2) \times U(1)$, is widely believed not to be the *ultima ratio*. The SM does not unify the electroweak and strong forces since the coupling constants of these interactions are different and appear to be independent. However, one should expect that in a more fundamental theory the three forces are described within a single gauge group and, hence, with only one coupling constant at high energy scales. This grand unified theory will be based on a gauge group containing $SU(3) \times SU(2) \times U(1)$ as a subgroup and it will be reduced to this symmetry at low energies.

Two predictions of grand unified theories may have interesting consequences in the energy range of a few hundred GeV [71]:

(a) The unified symmetry group must be spontaneously broken at the unification scale $\Lambda_{\rm GUT} \gtrsim 10^{16}$ GeV in order to be compatible with the experimental bounds on the proton lifetime. However, the breaking to the SM group may occur in several steps and some subgroups may remain unbroken down to a scale of order 1 TeV. In this case the surviving group factors allow for new gauge bosons with masses not far above the scale of electroweak symmetry breaking. Besides $SU(5)$, two other unification groups have received much attention: In $SO(10)$ three new gauge bosons $W_R^\pm, Z_R$ are predicted, while in $E(6)$ a light neutral Z' boson may exist in the TeV range.

The virtual effects of a new Z_R/Z' boson associated with the most general effective theories which arise from breaking $SO(10) \to SU(2)_L \times SU(2)_R \times U(1)$ and $E(6) \to SU(3) \times SU(2) \times U(1) \times U(1)_{Y'}$, have been investigated in Ref. [9]. Assuming the Z_R, Z' bosons to be heavier than the available c.m. energy, the propagator effects on various observables of the process

$$e^+e^- \xrightarrow{V} f\bar{f} \;: \quad V = \gamma, Z \text{ and } Z_R/Z'$$

have been studied in detail. As shown in Table 2, the effects of new vector bosons can be probed for masses up to 5 TeV at a 500 GeV collider. While they may be produced directly up to about 5 TeV at the LHC, experiments at the e^+e^- collider will measure the couplings of the vector bosons to fermions very precisely, thus identifying the physical nature of the new bosons. Masses up to 10 TeV and 50 TeV can be probed in e^+e^- colliders operating at 800 GeV and 5 TeV, respectively. These two windows extend to much higher scales than the direct discovery limits anticipated at LHC.

(b) The grand unification groups incorporate extended fermion representations in which a complete generation of SM quarks and leptons can be naturally embedded. These representations accommodate a variety of additional new fermions. It is conceivable that the new fermions acquire masses not much larger than the Fermi scale. This is necessary if the predicted new gauge bosons are relatively light. $SO(10)$ is the simplest group in which the 15 members of each SM generation of fermions can be embedded into a single multiplet. This representation has dimension **16** and contains a right–handed neutrino. The group $E(6)$ contains $SU(5)$ and $SO(10)$ as subgroups. In $E(6)$, each quark–lepton generation belongs to a representation of dimension **27**. To complete this representation, twelve new fields are needed in addition to the SM fermion fields. In each family the spectrum includes an additional isodoublet of leptons (N_E,E), two isosinglet neutrinos (N,n) and an isosinglet quark (D) with charge $-1/3$.

TABLE 2. *Sensitivity limits of Z_R masses in $SO(10)$ and Z' masses in $E(6)$ at e^+e^- linear colliders in the TeV range [9].*

$\sqrt{s}$	$SO(10)$	$E(6)$
500 GeV	6 TeV	5–7 TeV
800 GeV	10 TeV	8–11 TeV
5 TeV	$\sim$ 50 TeV	$\sim$ 50 TeV

If the new particles have non–zero electromagnetic and weak charges, and if their masses are smaller than the beam energy, they can be pair produced, $e^+e^- \to F\bar{F}$. In general, the production processes are built up by a superposition of s–channel γ and Z exchanges, but additional contributions could come from the extra neutral bosons if their masses are not much larger than the c.m. energy [71]. The cross sections are large, of the order of the point–like QED cross section. This gives rise to samples of several thousands of events. Fermion mixing, if large enough, leads to additional production mechanisms for the new fermions: single production in association with the light partners, $e^+e^- \to F\bar{f}$. In this case, masses very close to the total energy of the e^+e^- collider can be reached.

VI TOP QUARK PHYSICS AND QCD

Top quarks are the heaviest matter particles in the 3–family Standard Model. Introduced to incorporate CP violation in the left–handed charged–current sector, they may therefore hold the key for many aspects of physics beyond the Standard Model at high–energy scales [72]. Examples in which the large t mass is crucial, are multi–Higgs doublet models, models of dynamical symmetry breaking, compositeness and supersymmetry.

A Profile of the Top Quark

For a top mass larger than the W mass, the channel $t \to b + W^+$ is the dominant decay mode. For $\mathrm{m}_t \sim 175\,\mathrm{GeV}$ the width of the top quark, $\Gamma_t \sim 1.4\,\mathrm{GeV}$, is so large compared with the scale Λ of the strong interactions that this quark can be treated as a bare quantum which is not dressed by non–perturbative strong interactions [73]. Pair production [74,75] in $e^+e^- \to t\bar{t}$ is therefore a useful tool to study the properties of the top quark.

Chirality of the (tb) decay current: The precise determination of the weak isospin quantum numbers does not allow for large deviations of the (tb) decay current from the left–handed SM prescription. Nevertheless, since $V+A$ admixtures may grow with the masses of the quarks involved [through mixing with heavy mirror quarks, for instance], it is necessary to check the chirality of the decay current directly. The l^+ energy distribution in the semileptonic decay chain $t \to W^+ \to l^+$ depends on the chirality of the current. Any deviation from the standard $V-A$ current would lead to a stiffening of the spectrum and, in particular, to a non-zero value at the upper end–point of the energy distribution. A sensitivity of about 1 % to a possible $V+A$ admixture can be reached experimentally [9].

Magnetic dipole moments: If the electrons in $e^+e^- \to t\bar{t}$ are left–handedly polarized, the top quarks are produced preferentially as left–handed particles in the forward direction while only a small fraction is produced as right–handed particles in the backward direction [76], so that the backward direction is most sensitive to small anomalous magnetic moments of the top quarks. The anomalous magnetic moments can be bounded to the per–cent level by measuring the angular dependence of the t quark cross section in this region.

Electric dipole moments: These moments are generated by CP–non invariant interactions. Non–zero values of the moments can be detected through non–vanishing expectation values of CP–odd momentum tensors such as $T_{ij} = (n_+ - n_-)_i (n_+ \times n_-)_j$ with $n_\pm$ being the unit momentum vectors of the W decay leptons. Sensitivity limits to γ, Z electric dipole moments of $\lesssim 10^{-18}$ e cm can be reached [77,9] for an integrated luminosity of $\int \mathcal{L} = 100$ fb^{-1} at $\sqrt{s} = 500\,\mathrm{GeV}$.

B The Top Mass and QCD

Quark–antiquark production near the threshold in e^+e^- collisions is of exceptional interest. The long time which the particles stay close together at low velocities, allows the strong interactions to build up remnant structures of toponium bound states and resonances, smeared out as a result of the rapid top decay: The decay time of the states becomes shorter than the revolution time of the constituents so that sharp toponium states cannot be formed any more. The remnants nevertheless induce a steep rise of the excitation curve near the threshold.

Since the rapid t decay restricts the interaction region to small distances, the excitation curve can be predicted in perturbative QCD [78], based essentially on the Coulombic interquark potential $V(R) = -4/3 \times \alpha_s(R)/R$. The cross section is built up by the superposition of all $nS(t\bar{t})$ states. The form and the height of the excitation curve are very sensitive to the mass of the top quark.

Detailed experimental simulations predict the following sensitivity to the top mass [9] : $\delta m_t \lesssim 200\,\mathrm{MeV}$ for an integrated luminosity of $\int \mathcal{L} = 50$ fb^{-1}, remnant uncertainties due to higher–order QCD corrections and experimental errors contributing at an approximately equal amount. At proton colliders a sensitivity of about 2 GeV has been claimed for the top mass, based on the reconstruction of top quarks from jet and lepton final states. Thus, e^+e^- colliders will improve the measurement of the top quark mass by at least an order of magnitude.

Measurements of the $t\bar{t}$ excitation curve near the threshold can also be used to determine the QCD coupling α_s with an error similar to present measurements. Jet analyses in the hadronic final states of e^+e^- annihilation can be exploited to extend the high-energy scale at which α_s is measured. In the GigaZ mode however significant improvements on the accuracy of the α_s determination can be expected which reduce the error of $\alpha_s(M_Z^2)$ to a level of $1 \cdot 10^{-3}$ [9].

REFERENCES

1. S.L. Glashow, Nucl. Phys. 20 (1961) 579; S. Weinberg, Phys. Rev. Lett. 19 (1967) 1264; A. Salam, in Elementary Particle Theory, *ed.* N. Svartholm (Almqvist and Wiksells, Stockholm 1968).
2. H. Fritzsch and M. Gell-Mann, Proc. XVI Int. Conf. on High Energy Physics, *eds.* J.D. Jackson and A. Roberts, (Fermilab 1972).
3. P.W. Higgs, Phys. Rev. Lett. 12 (1964) 132; Phys. Rev. 145 (1966) 1156; F. Englert and R. Brout, Phys. Rev. Lett. 13 (1964) 321; G.S. Guralnik, C.R. Hagen and T.W. Kibble, Phys. Rev. Lett. 13 (1964) 585.
4. J.C. Pati and A. Salam, Phys. Rev. D10 (1974) 275; H. Georgi and S. Glashow, Phys. Rev. Lett. 32 (1974) 438; H. Fritzsch and P. Minkowski, Ann. Phys. 93 (1975) 193.
5. J. Wess and B. Zumino, Nucl. Phys. B70 (1974) 39.
6. H. Murayama and M.E. Peskin, Ann. Rev. Nucl. Part. Sci. 46 (1996) 553.
7. E. Accomando et al., Phys. Rep. 299 (1998) 1, [hep–ph/9705442].
8. P.M. Zerwas, Proceedings, 1999 Cargèse Lectures, hep–ph/0003221.
9. TESLA TDR, EDFA/DESY Workshop, http://www.desy.de/ lcnotes/tdr/.
10. American LC WG, hep–ex/0007022; FNAL LC WG, P. Derwent et al., unpublished.
11. http://clicphysics.web.cern.ch/CLICphysics/.
12. P. Grannis, Summary Report, these proceedings, [hep–ex/0101001].
13. Y. Okada; K. Desch, these proceedings.
14. M. Battaglia, these proceedings.
15. N. Cabibbo, L. Maiani, G. Parisi and R. Petronzio, Nucl. Phys. B158 (1979) 295; K. Riesselmann, DESY 97–222, [hep–ph/9711456].
16. LEPEWWG, http://lepewwg.web.cern.ch/LEPEWWG.
17. M. Veltman, Acta Phys. Polon. B8 (1977) 475.
18. R. Barbieri and A. Strumia, Phys. Lett. B462 (1999) 144.
19. J. Bagger, A. Falk and M. Swartz, Phys. Rev. Lett. 84 (2000) 1385.
20. R. Barate et al, Phys. Lett. B495 (2000) 1; M. Acciari et al, Phys. Lett. B495 (2000) 18; P. Igo-Kemenes, LEPC Session, CERN, Nov.3, 2000.
21. J. Ellis, M.K. Gaillard and D.V. Nanopoulos, Nucl. Phys. B106 (1976) 292; B.L. Ioffe and V.A. Khoze, Sov. J. Part. Nucl. 9 (1978) 50; B.W. Lee, C. Quigg and

H.B. Thacker, Phys. Rev. D16 (1977) 1519; D.R.T. Jones and S.T. Petcov, Phys. Lett. B84 (1979) 440.

22. M. Spira and P.M. Zerwas, Proceedings, 36. Int. Universitätswochen, Schladming 1997, hep–ph/9803257.
23. V. Barger, K. Cheung, A. Djouadi, B.A. Kniehl and P.M. Zerwas, Phys. Rev. D49 (1994) 79.
24. D.J. Miller, S.Y. Choi, B. Eberle, M. Mühlleitner and P.M. Zerwas, Report DESY 01-010; D.J. Miller, these proceedings; A. Para, private communication.
25. A. Djouadi, J. Kalinowski and P.M. Zerwas, Z. Phys. C54 (1992) 255; S. Dawson and L. Reina, Phys. Rev. D59 (1999) 054012; S. Dittmaier et al., Phys. Lett. B 441 (1998) 383.
26. A. Djouadi, W. Kilian, M. Mühlleitner and P. Zerwas, Eur. Phys. J. C10 (1999) 27.
27. D.J. Miller and S. Moretti, Eur. Phys. J. C13 (2000) 459.
28. C. Castanier, P. Gay, P. Lutz and J. Orloff, these proceedings, [hep–ex/0101028].
29. J.F. Gunion and H.E. Haber, Nucl. Phys. B272 (1986) 1 and B278 (1986) 449.
30. A. Djouadi, J. Kalinowski, P. Ohmann and P.M. Zerwas, Z. Phys. C74 (1997) 93.
31. M. Mühlleitner, M. Kramer, M. Spira and P.M. Zerwas, Report DESY 00-192, [hep–ph/0101083].
32. J.R. Espinosa and J.F. Gunion, Phys. Rev. Lett. 82 (1999) 1084.
33. B. Dobrescu; W. Kilian, these proceedings, [hep–ph/0012243].
34. T. Appelquist and C. Bernard, Phys. Rev. D22, 200 (1980); A. Longhitano, Phys. Rev. D22 (1980) 1166; Nucl. Phys. B188 (1981) 118; T. Appelquist and G.-H. Wu, Phys. Rev. D48 (1993) 3235; M. Veltman, Report CERN 97–05.
35. E. Boos, H.-J. He, W. Kilian, A. Pukhov, C.-P. Yuan and P.M. Zerwas, Phys. Rev. D57 (1998) 1553 and Phys. Rev. D61 (2000) 077901.
36. V. Barger, K. Cheung, T. Han and R.J. Phillips, Phys. Rev. D52 (1995) 3815.
37. A. DeRoeck, these proceedings.
38. R. Casalbuoni, A. Deandrea, S. DeCurtis, D. Dominici, R. Gatto and J.F. Gunion, JHEP 9908 (1999) 011.
39. J.L. Feng, K.T. Matchev and T. Moroi, Phys. Rev. D61 (2000) 075005.
40. M. Drees, LC-Note, hep-ph/0101217.
41. M. Carena, M. Quiros, A. Riotto, I. Vilja and C. Wagner, Nucl. Phys. B503 (1997) 387.
42. R. Godbole, these proceedings.
43. M. Peskin, Lecture, EPS HEP99, Tampere 1999, [hep–ph/0002041].
44. G. Blair, W. Porod and P.M. Zerwas, Phys. Rev. D63 (2001) 017703; G. Blair, these proceedings, [hep-ph/0011367].
45. U. Martyn, these proceedings.
46. S.Y. Choi, A. Djouadi, M. Guchait, J. Kalinowski, H.S. Song and P.M. Zerwas, Eur. Phys. J. C14 (2000) 535.
47. G. Moortgat-Pick, H. Fraas, A. Bartl and W. Majerotto, Eur. Phys. C7 (1999) 113.
48. A. Bartl, H. Eberl, S. Kraml, W. Majeroko and W. Porod, EPJdirect C6 (2000) 1.
49. J. Kalinowski, these proceedings, [hep–ph/0101111].
50. U. Martyn and G.A. Blair, hep–ph/9910416.
51. J. Kneur and G. Moultaka, Phys. Rev. D59 (1999) 015005 and D61 (2000) 075004.

52. V. Barger, T. Falk, T. Han, J. Jiang, T. Li and T. Plehn, MADPH-00-1207, [hep–ph/0101090].
53. A.H. Chamseddine, R. Arnowitt and P. Nath, Phys. Rev. Lett. 49 (1982) 970; R. Barbieri, S. Ferrara and C.A. Savoy, Phys. Let. B119 (1982) 343.
54. Z. Chacko, M. Luty, A. Nelson and E. Ponton, JHEP 0001 (2000) 003; M. Schmaltz and W. Shiba, Phys. Rev. D59 (1999) 086004.
55. M. Dine, A. Nelson and Y. Shirman, Phys. Rev. D51 (1995) 1362; M. Dine, A. Nelson, Y. Nir and Y. Shirman, Phys. Rev. D53 (1996) 2658; G.F. Giudice and R. Rattazzi, CERN Report, hep–ph/9801271.
56. G.F. Giudice, M.A. Luty, H. Murayama and R. Rattazzi, JHEP 9812 (1998) 027.
57. P. Binétruy, M.K. Gaillard and B.D. Nelson, LBNL-46970, [hep–ph/0011081].
58. J. Scherk and J.H. Schwarz, Nucl. Phys. B153 (1979) 61.
59. T. Tsukamoto, K. Fujii, H. Murayama, M. Yamaguchi and Y. Okada, Phys. Rev. D51 (1995) 3153.
60. N. Arkani-Hamed, these proceedings.
61. N. Arkani-Hamed, S. Dimopoulos and G. Dvali, Phys. Lett. B429 (1998) 263; and Phys. Rev. D59 (1999) 086004.
62. G.F. Giudice, R. Rattazzi and J.D. Wells, Nucl. Phys. B544 (1999) 3.
63. E. Mirabelli, M. Perelstein and M. Peskin, Phys. Rev. Lett. 82 (1999) 2236.
64. T. Han, J. Lykken and R.J. Zhang, Phys. Rev. D59 (1999) 105006; J.L. Hewett, Phys. Rev. Lett. 82 (1999) 4765; T.G. Rizzo, Phys. Rev. D59 (1999) 115010.
65. T. Rizzo, these proceedings; and private communication.
66. L. Randall and R. Sundrum, Phys. Rev. Lett. 83 (1999) 3370 and 4690.
67. R. Hawkings and K. Mönig, EPJdir. C8 (1999) 1.
68. K. Mönig, these proceedings, [hep–ex/0101005].
69. J. Erler, S. Heinemeyer, W. Hollik, G. Weiglein and P.M. Zerwas, Phys. Lett. B486 (2000) 125.
70. W.J. Stirling and A. Werthenbach, Eur. Phys. J. C14 (2000) 103.
71. A. Djouadi, Proceedings, *Workshop on Physics and Experiments with e^+e^- Linear Colliders*, (Iwate 1995); C.S. Kim, these proceedings.
72. L. Orr; S. Magill, these proceedings.
73. I.I. Bigi, Y.L. Dokshitzer, V. Khoze, J. Kühn and P.M. Zerwas, Phys. Lett. 181B (1986) 157.
74. J. Jersak, E. Laermann and P.M. Zerwas, Phys. Rev. D25 (1982) 363.
75. K. Chetyrkin, J. Kühn and M. Steinhauser, Nucl. Phys. B482 (1996) 213.
76. M.E. Peskin and C. Schmidt, Proceedings, *Physics and Experiments with e^+e^- Linear Colliders*, (Saariselkä 1991).
77. W. Bernreuther et al., Proceedings, *e^+e^- Collisions at 500 GeV: The Physics Potential, ed.* P.M. Zerwas, (Munich–Annecy–Hamburg 1991/93), DESY 92–123A+B, 93–123C.
78. A.H. Hoang, M. Beneke, K. Melnikov, T. Nagano, A. Ota, A.A. Penin, A.A. Pivovarov, A. Signer, V.A. Smirnov, Y. Sumino, T. Teubner, O. Yakovlev and A. Yelkhovsky, EPJdirect C3 (2000) 1.